Available online at www.sciencedirect.com
ScienceDirect
Trans. Nonferrous Met. Soc. China 25(2015) 457−464
Transactions of Nonferrous Metals Society of China
www.tnmsc.cn

Thermal properties of glass-ceramic bonded thermal barrier coating system

S. GHOSH

Bio-ceramics and Coating Division, CSIR–Central Glass and Ceramic Research Institute, Kolkata 700032, India

Received 26 March 2014; accepted 18 August 2014

Abstract: The thermal properties of a thermal barrier coating (TBC) system comprised of BaO–MgO–SiO_2 based glass-ceramic bond coating, 8% (mass fraction) yttria stabilized zirconia (8YSZ) top coating and nimonic alloy substrate were evaluated. The thermal diffusivity and thermal conductivity of the TBC coated substrate were lower than those of bare substrate and glass-ceramic coated substrate under identical conditions. The specific heat capacity, thermal diffusivity and thermal conductivity of the TBC coated substrate increase with the increase of the temperature. Further, it is observed that the thermal conductivity of the TBC system decreases with the increase in the top coating thickness.

Key words: glass-ceramic coating; thermal barrier coating; thermal properties; yttria stabilized zirconia

1 Introduction

Thermal barrier coatings (TBCs) are widely applied to protect the hot-section components of modern gas turbine engine from the aggressive environments. The oxidation resistance, thermal shock resistance and thermal insulation capacity of the TBCs are of primary importance among their thermo-mechanical properties related to the high temperature applications [1]. The basic function of a TBC is to restrict the heat transfer from the hot gas in the engine to the surface of the coated alloy component [2].

Generally, TBC system consists of a ceramic top coating, a metallic bond coating and a metallic substrate [3]. Usually, M-NiCrY type bond coating is applied to assist the adherence and stress relaxation. However, exposure of the TBC system to elevated temperatures leads to the development of a thermally grown oxide (TGO) layer between the bond coating and top coating [4]. TGO has a major influence on the TBC durability. As the TGO layer thickness increases with the operation time, high stresses are generated at the bond coating/TGO interface due to the volume increase, thermal expansion misfit and applied loads. As a consequence, crack initiates and propagates, leading to the spallation of the ceramic top coating, finally resulting in the failure of the TBC system [4,5]. Thus, the bond coating is the most critical component of the TBC system. The chemistry and microstructure of bond coating affect the durability through the structure and morphology of the developed TGO [6,7].

Glass-ceramic coatings possess excellent chemical inertness, low thermal conductivity, high temperature stability and superior mechanical properties. Because of the excellent combination of these properties, glass-ceramic coatings can efficiently be utilized to reduce high temperature degradation of the structural materials [8]. Further, glass-ceramic coating is also conceived as cheap but effective alternative thermal barrier coating. 3% yttria doped zirconia dispersed in a high temperature resistant alumino-borosilicate glassy phase showed good performance as a thermal barrier coating [9]. The inherent low thermal conductivity of the glass-ceramic based bond coating can reduce the metal substrate temperature and thereby protect the substrate from oxidation and creep failure. Therefore, glass-ceramics may be an ideal bond coating in a TBC system. Potential of glass-ceramics as good oxidation and thermal shock resistant bond coating in the conventional thermal barrier coating system has been already established [10,11].

The thermal properties of the TBCs have been extensively studied by the researchers as these coatings are used at the elevated temperatures [12–17]. The thermal insulation property of the TBCs is determined by their thermal conductivity, which plays an important role in the heat transfer processes [14]. In the present work, an attempt was made to carry out in-depth study for the

Corresponding author: S. GHOSH; Tel: +91-33-2473-3469/76/77/96; Fax: +91-33-473-0957; E-mail: sumana@cgcri.res.in
DOI: 10.1016/S1003-6326(15)63624-X

evaluation of thermal conductivity of a glass-ceramic bonded TBC system.

2 Experimental

BaO−MgO−SiO_2 based glass-ceramic coating (thickness ~100 μm) was applied on the nimonic alloy (AE 435) substrate by conventional enameling technique. The glass and substrate composition has been reported elsewhere [10]. Nimonic alloy substrate with dimensions of 10 mm × 10 mm × 2 mm was used for the present work. 8% YSZ (8YSZ) powder was air plasma sprayed on the glass-ceramic coated substrates using a METCO-F4 plasma gun. The thermal spraying parameters for YSZ top coating are shown in Table 1 and the porosity of YSZ coating is 8%−12%. The thickness of 8YSZ top coating varies from 200 μm to 400 μm.

Table 1 Thermal spraying parameters for YSZ top coating porosity of YSZ coating

Spraying parameters	Value
Powder injection	Outside nozzle 6 mm
Power input/kW	40
Primary (Ar)/secondary (H_2) gas flow in plasma/(L·min^{-1})	35, 10
Carrier gas (Ar) flow in feeder nozzle/(L·min^{-1})	2.6
Stand-off distance/mm	120

Laser-flash technique was utilized to measure the specific heat capacity and thermal diffusivity of the uncoated, glass-ceramic and TBC coated substrates as a function of temperature using a thermal diffusivity measuring system (FLASHLINE^{TM}4010, Anter Corporation, USA). High intensity laser pulse (Nd:glass laser, average pulse width −300 μs) was absorbed at the front surface of the specimen and the temperature increase of the rear surface was measured by a thermocouple (type S thermocouple). The thermal diffusivity was determined by the shape of the temperature versus time curve at the rear surface. The specific heat capacity was determined by the maximum temperature indicated by the thermocouple and the thermal conductivity was estimated by the product of the thermal diffusivity, specific heat capacity and density [17]. Thermal diffusivity measurements were made in a vacuum chamber from the room temperature to 1000 °C. Prior to application of the laser pulse, the specimen was coated with gold and subsequently with graphite thin films on the surfaces on which the heating was conducted by the laser pulse and temperature increment was monitored. Coating was necessary to absorb the laser pulse. Coating also ensures the heat flow by conduction method.

3 Results and discussion

3.1 Microstructural characterization

Figure 1 shows the surface microstructures of nimonic alloy substrate, glass-ceramic bond coating and 8YSZ top coating. It can be seen that the surface microstructures of substrate, bond coating as well as top coating are almost devoid of any defects like pores and microcracks. Figure 2 demonstrates the fractured cross-sectional micrographs of 8YSZ top coating. The cross-sectional images show the single splat, splat/splat interface, inter-lamellar pore, globular pore, intra-splat crack and columnar structure of the top coating. Based on the microstructural observations, small pores and cracks are presented in the top coating.

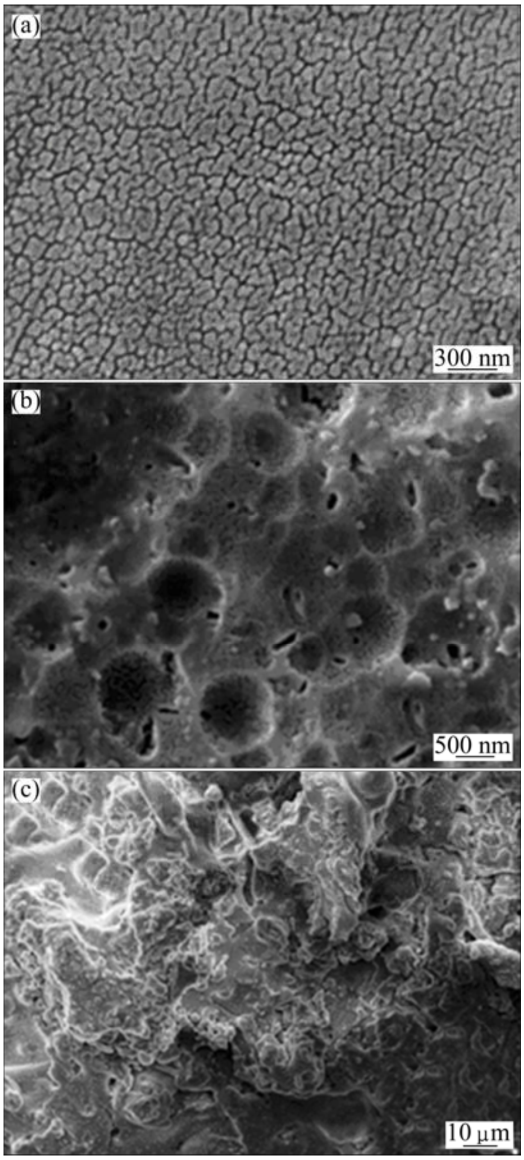

Fig. 1 SEM images of substrate (a), glass-ceramic bond coating (b) and 8YSZ top coating (c)

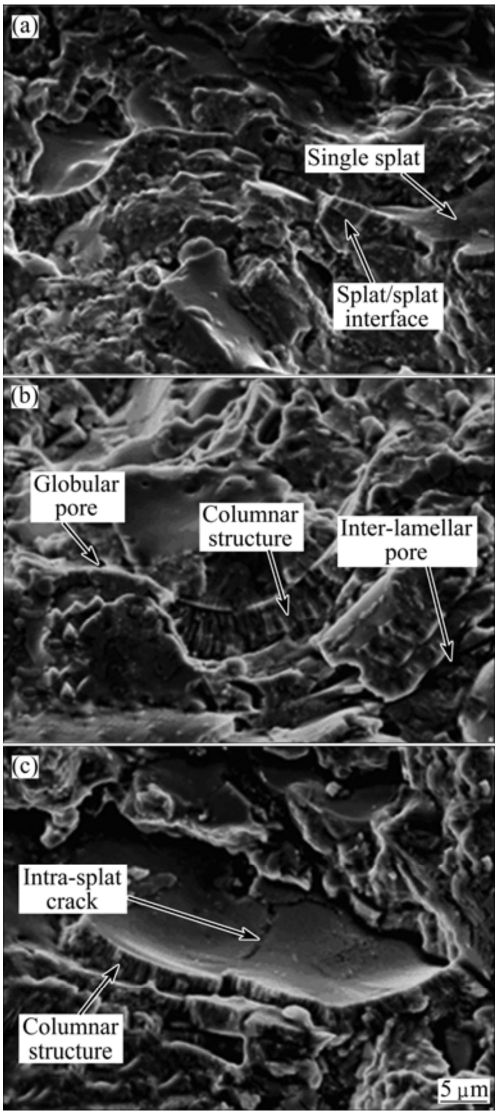

Fig. 2 Fractured cross-sectional micrographs of 8YSZ top coating: (a) Single splat, splat/splat interface; (b) Inter-lamellar pore, globular pore, columnar structure; (c) Intra-splat crack, columnar structure

3.2 Measurement of specific heat capacity, thermal diffusivity and thermal conductivity

The thermal diffusivity (α) was determined by the following equation (1) [17]:

$$\alpha=1.38L^2/\Pi^2 t_{1/2} \quad (1)$$

where L is the thickness of specimen and $t_{1/2}$ is the time required for the rear surface to reach half of the maximum temperature rise. From Eq. (1), it is clear that the thickness of specimen is very important for the calculation of thermal diffusivity. Specific heat capacity measurements were done by comparing the temperature rise in the specimen with that in molybdenum standard material [17]. Same amount of laser energy falls on both the samples. Thus, we have [18]

$$E_T = mc\Delta\theta = m_s c_s \Delta\theta_s \quad (2)$$

where E_T is the total laser energy; m is the mass of the specimen; c is the specific heat capacity of the specimen; $\Delta\theta$ is the temperature rise of the specimen; m_s, c_s and $\Delta\theta_s$ are the respective mass, specific heat capacity and rise of temperature of the standard specimen, respectively. The thermal conductivities of the uncoated, glass-ceramic coated and TBC coated substrates were calculated according to [17,19]:

$$k=\alpha c\rho \quad (3)$$

where k is the thermal conductivity; α is the thermal diffusivity; ρ is the density of the material.

3.3 Thermal conductivity of substrate

The thermal conductivity of the nimonic alloy substrate was calculated by putting the measured thermal diffusivity, specific heat capacity and density values in Eq. (3). The density of the substrate was measured by the Archimedes method and found out to be 8.79 g/cm^3. The specific heat capacity, thermal diffusivity and thermal conductivity values of the substrate with respect to temperature are shown in Figs. 3. The specific heat capacity, thermal diffusivity and thermal conductivity values at 200−1000 °C were found to be in the range of 0.421−0.596 W·s/(g·K), 0.0421−0.0526 cm^2/s, 15.58−27.56 W/(m·K), respectively. It is further observed that the specific heat capacity, thermal diffusivity and thermal conductivity values increased with the increase of the temperature. The thermal diffusivity of the substrate material increases with the increase in temperature due to the absence of large amount of imperfections like porosity and microcracks in the substrate [12,16], as can be seen from the surface microstructure (Fig. 1(a)). It is assumed that the number of free electrons increases with increasing the temperature. Movement of free electrons has a dominant effect on the thermal conductivity than phonons up to 1000 °C. Thus, the thermal conductivity of nimonic alloy substrate increases with the increase in temperature [20].

3.4 Thermal conductivity of glass-ceramic coated substrate

The density of the glass-ceramic coated substrate was measured to be 8.63 g/cm^3 by the Archimedes method. Figures 4(a)−(c) show the specific heat capacity, thermal diffusivity and thermal conductivity values of the glass-ceramic coated substrate as a function of temperature. At 200−1000 °C, the specific heat capacity, thermal diffusivity and thermal conductivity values of the composite are found to be 0.406−0.582 W·s/(g·K), 0.0354−0.0465 cm^2/s and 12.40−23.36 W/(m·K), respectively. It is noted that the specific heat capacity, thermal diffusivity and thermal conductivity values increase with the increase in temperature. The increase in

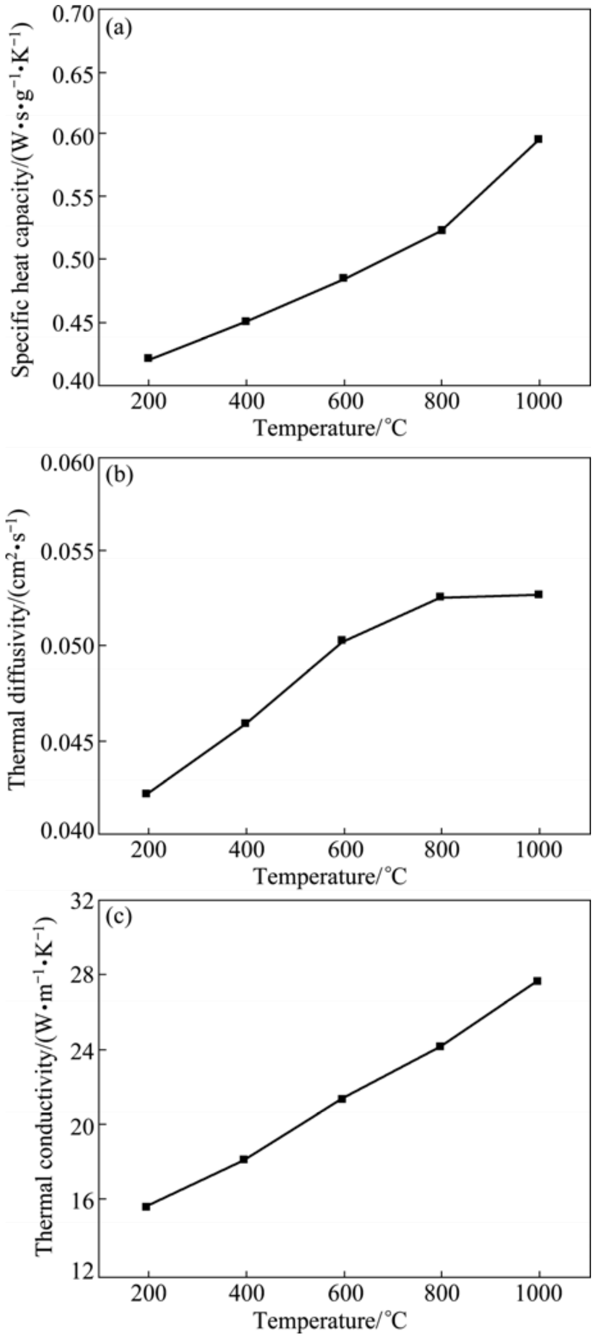

Fig. 3 Specific heat capacity (a), thermal diffusivity (b) and thermal conductivity (c) versus temperature curves of nimonic alloy substrate

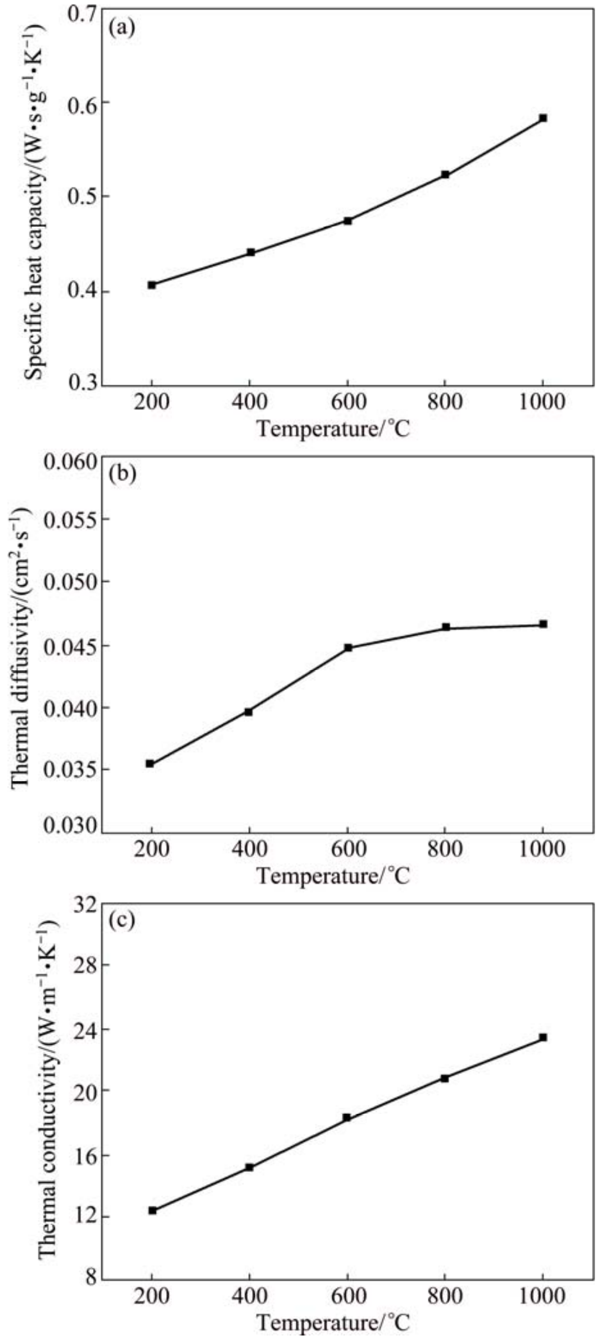

Fig. 4 Specific heat capacity (a), thermal diffusivity (b), and thermal conductivity (c) versus temperature curves of glass-ceramic coated substrate

the thermal diffusivity with the increase of the temperature up to 1000 °C can be ascribed to the presence of low amount of pores, microcracks and any other defects in the glass-ceramic bond coating [12,16]. The thermal conductivity in glass-ceramic materials depends on the partial conductivities and volume fractions of the constituting phases, structural parameters of crystallites and the interstitial material between them [21]. Therefore, the thermal conductivity increment as a function of temperature may be attributed to high partial conductivities of the glassy phase as well as glass-ceramic phase. The relaxation rate increases in the glass-ceramic bond coating with increasing temperature from 200 to 1000 °C because of increasing mobility of the ions [21]. Further, sintering related phenomena are accountable for the increase of thermal conductivity as a function of temperature [12]. Further, it may be noted that the thermal conductivity values of the glass-ceramic coated substrate are lower than those obtained for the bare substrate in the temperature range of 200−1000 °C. The thermal conductivity of the glass-ceramic bond coating is calculated using [19]

$$k_a = \frac{k_s k_{bc}}{k_s t_{bc} + k_{bc} t_s} \tag{4}$$

where k_a is the thermal conductivity of the glass-ceramic coated substrate; k_s is the thermal conductivity of the substrate; k_{bc} is the thermal conductivity of the glass-ceramic bond coat; t_{bc} and t_s are the thickness fractions of the glass-ceramic bond coat and the substrate, respectively. Figure 5 shows the thermal conductivity of the glass-ceramic bond coating as a function of temperature. It can be observed that the glass-ceramic bond coating has lower thermal conductivity (5.757 W/(m·K) at 1000 °C) than that (27.56 W/(m·K) at 1000 °C) of the substrate. Hence, the glass-ceramic coated substrate shows lower thermal conductivity than the bare substrate.

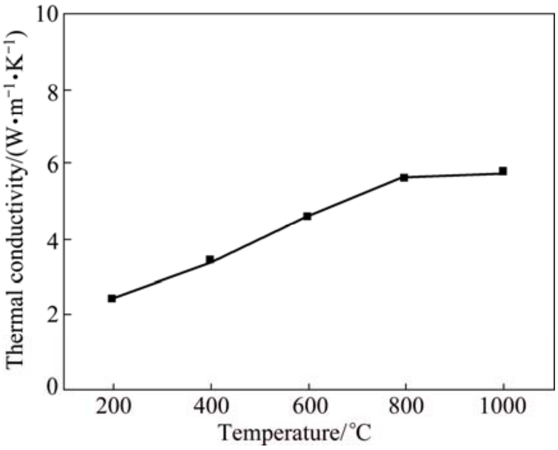

Fig. 5 Thermal conductivity versus temperature curve of glass-ceramic bond coating

3.5 Thermal conductivity of TBC coated substrate

The TBC coated substrate with ~100 μm glass-ceramic bond coating and ~200 μm 8YSZ top coating was used for thermal diffusivity and specific heat capacity measurements. The density of the TBC coated substrate is measured to be 7.74 g/cm^3 by the Archimedes method. Figure 6 shows the specific heat capacity, thermal diffusivity and thermal conductivity values of the TBC (~300 μm thickness) coated substrate as a function of temperature. At 200−1000 °C, the specific heat capacity, thermal diffusivity and thermal conductivity values are in the range of 0.458−0.603 W·s/(g·K), 0.0346−0.0462 cm^2/s and 12.27−21.56 W/(m·K), respectively. It can be noted that the specific heat capacity, thermal diffusivity and thermal conductivity values of the TBC coated substrate increase with the increase in temperature. The increase in thermal diffusivity as a function of temperature can be explained by the heat transfer mechanism. At high temperatures up to 1000 °C, the heat transfer in 8YSZ top coating mainly occurs depending on the phonon conductivity, which is influenced by the microstructural features of the top coating (e.g., porosity and microcracks). In the case of the present TBC system, the thermal diffusivity of the TBC coated substrate increases with increasing the temperature because of lack of porosity, microcracks or any other imperfections in the top coating and bond coating [12,16]. The increase in thermal conductivity of TBC coated substrates with increasing the temperature is mainly caused by the sintering based phenomena in the top coating as well as in the bond coating [12].

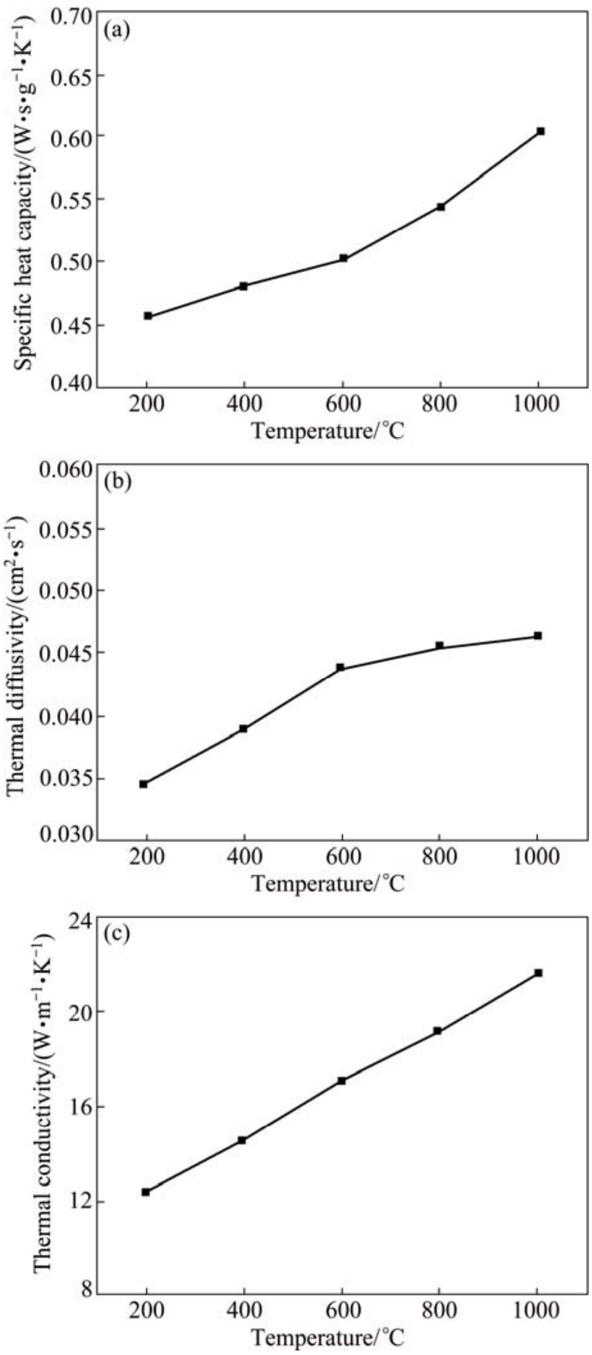

Fig. 6 Specific heat capacity (a), thermal diffusivity (b) and thermal conductivity (c) versus temperature curves of TBC (~300 μm thickness) coated substrate

The thermal conductivity values of the TBC coated substrate with ~100 μm thickness glass-ceramic bond coating and ~400 μm 8YSZ top coating are further improved under identical conditions. The density of the TBC (thickness ~500 μm) coated substrate is measured to be 7.51 g/cm^3 by the Archimedes method. Figure 7 shows the specific heat capacity, thermal diffusivity and thermal conductivity values of the ~500 μm TBC coated substrate as a function of temperature. At 200−1000 °C, the specific heat capacity, thermal diffusivity and thermal conductivity values of this TBC system are in the range of 0.558−0.743 W·s/(g·K), 0.0179−0.0308 cm^2/s and 7.50−17.19 W/(m·K), respectively. It can be noted that the thermal conductivity values of the TBC coated substrates are lower than those of the substrate and the glass-ceramic coated substrate under identical conditions. Further, it is observed that the thermal conductivity of the TBC system decreases with increasing the thickness of the top coating. With the increase of the thickness of top coating from 200 to 400 μm, the thermal conductivity value of the TBC system decreases from 21.56 to 17.19 W/(m·K) at 1000 °C under identical conditions.

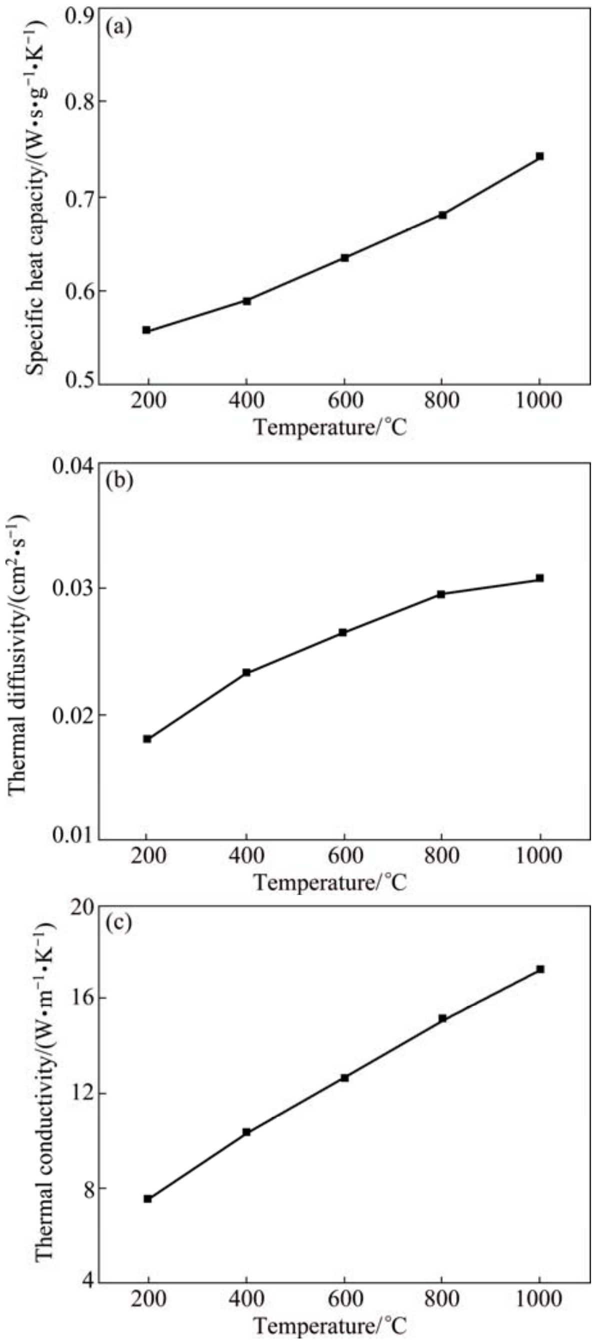

Fig. 7 Specific heat capacity (a), thermal diffusivity (b) and thermal conductivity (c) versus temperature curves of TBC (~500 μm thickness) coated substrate

The thermal conductivity of the 8YSZ top coating is estimated using [19]

$$k_{\rm b}=\frac{k_{\rm a}k_{\rm tc}}{k_{\rm a}t_{\rm tc}+k_{\rm tc}t_{\rm a}} \tag{5}$$

where $k_{\rm b}$ is the thermal conductivity of the TBC system; $k_{\rm a}$ is the thermal conductivity of the glass-ceramic coated substrate; $k_{\rm tc}$ is the thermal conductivity of the top coating; $t_{\rm tc}$ and $t_{\rm a}$ are the thickness fractions of the top coating and the glass-ceramic coated substrate, respectively.

Figure 8 shows the calculated thermal conductivity of the 8YSZ top coat versus temperature curves. The thermal conductivity of ~200 μm thickness 8YSZ top coating initially decreases slightly with increasing temperature up to 800 °C (Fig. 8(a)). This might occur because the thermal diffusivity of the 8YSZ top coat decreases marginally with the increase in temperature due to the presence of some processing induced defects in the coating other than porosity [12]. Further, the densification of the 8YSZ top coating dominates over the thermal diffusivity decrement that leads to the overall increase of the thermal conductivity at 1000 °C [12]. In addition to the sintering phenomenon in the top coating, the relative deficiency of microcracks, porosity or any other defects in the ~400 μm 8YSZ top coating as compared to that in the ~200 μm 8YSZ top coating is probably responsible for the increase in thermal diffusivity as a function of temperature [12,16] and thereby, increasing the thermal conductivity of ~400 μm YSZ top coating with increasing temperature (Fig. 7(b)).

From Fig. 8, the top coating of 200 μm thickness has lower thermal conductivity (11.78 W/(m·K) at 1000 °C) than that (23.36 W/(m·K) at 1000 °C) of the glass-ceramic coated substrate. Further, ~400 μm 8YSZ top coating has much lower thermal conductivity (7.2 W/(m·K) at 1000 °C) than that (23.36 W/(m·K) at 1000 °C) of the glass-ceramic coated substrate. Therefore, when 8YSZ top coating is applied on the glass-ceramic coated substrate, the thermal conductivity of the TBC system decreases. With increasing the thickness of 8YSZ top coating, the thermal conductivity of the TBC system further decreases. Although 8YSZ has low thermal conductivity, yet further reduction in thermal conductivity of the TBC coated substrate is caused by existing porosity and cracks in the TBC and thermal resistance at the splat-splat interface in the top coating, bond coating/top coating interface and bond coating/substrate interface [19].

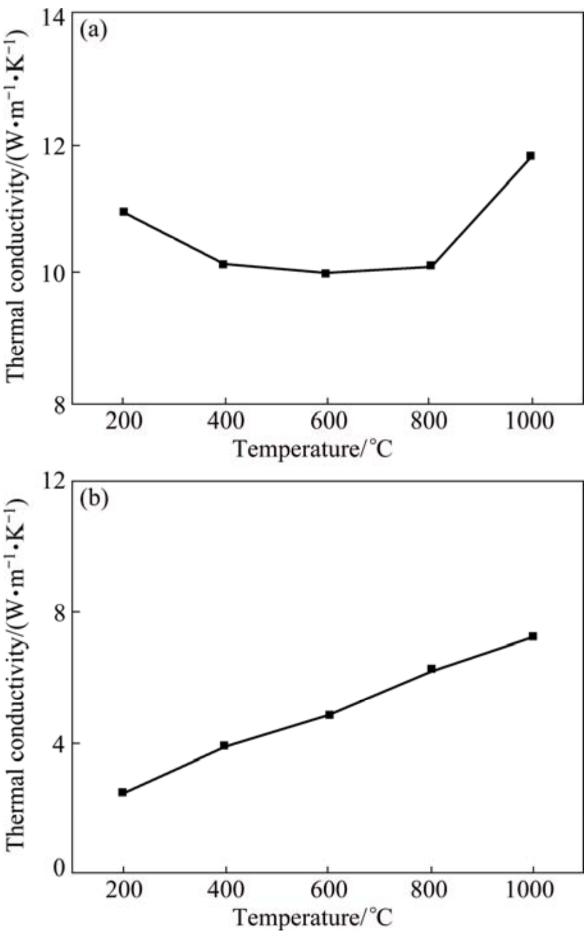

Fig. 8 Thermal conductivity versus temperature curves of 200 μm thick top coating (a) and 400 μm thick top coating (b)

4 Conclusions

1) Thermal conductivity property of a glass-ceramic bonded TBC system is quite satisfactory.

2) Thermal conductivity values of the nimonic alloy substrate, glass-ceramic coated substrate and TBC (thickness ~500 μm) coated substrate are 27.56, 23.36 and 17.19 W/(m·K) at 1000 °C, respectively.

3) The specific heat capacity, thermal diffusivity and thermal conductivity values of the bare substrate, glass-ceramic coated substrate and TBC coated substrate increase with the increase in temperature.

4) The thermal conductivity of the TBC coated substrate decreases with increasing the thickness of 8YSZ top coating.

Acknowledgements

The authors are grateful to Mr. K. DASGUPTA, Director, CSIR–Central Glass and Ceramic Research Institute (CSIR–CGCRI), Kolkata–700 032, India, for his kind permission to publish this work.

References

[1] BAI Y, ZHAO L, TANG J J, MA S Q, DING C H, YANG J F, YU L, HAN Z H. Influence of original powders on the microstructure and properties of thermal barrier coatings deposited by supersonic atmospheric plasma spraying, part II: Properties [J]. Ceramics International, 2013, 39: 4437−4448.

[2] CLARKE D R, LEVI C G. Materials design for the next generation thermal barrier coatings [J]. Annual Review of Materials Research, 2003, 33: 383−417.

[3] MARTENA M, BOTTO D, FINO P, SABBADINI S, GOLA M M, BADINI C. Modelling of TBC system failure: Stress distribution as a function of TGO thickness and thermal expansion mismatch [J]. Engineering Failure Analysis, 2006, 13: 409−426.

[4] GOSWAMI B, ROY A K, SAHAY S K. Thermal barrier coating system for gas turbine application—A review [J]. High Temperature Materials Processes, 2004, 23: 73−92.

[5] CHEN W R, WU X, MARPLE B R, PATNAIK P C. Oxidation and crack nucleation/growth in an air-plasma-sprayed thermal barrier coating with NiCrAlY bond coat [J]. Surfance & Coatings Technology, 2005, 197: 109−115.

[6] EVANS A G, MUMM D R, HUTCHINSON J W, MEIER G H, PETTIT F S. Mechanisms controlling the durability of thermal barrier coatings [J]. Progress in Materials Science, 2001, 46: 505−553.

[7] SCHLICHTING K W, PADTURE N P, JORDAN E H, GELL M. Failure modes in plasma-sprayed thermal barrier coatings [J]. Materials Science and Engineering A, 2003, 342: 120−130.

[8] DATTA S. Studies on broad spectrum corrosion resistant oxide coatings [J]. Bulletin of Materials Science, 2001, 24: 569−577.

[9] MAJUMDAR A, JANA S. Yttria doped zirconia in glassy matrix useful for thermal barrier coating [J]. Materials Letters, 2000, 44: 197−202.

[10] DAS S, DATTA S, BASU D, DAS G C. Glass–ceramics as oxidation resistant bond coat in thermal barrier coating system [J]. Ceramics International, 2009, 35: 1403−1406.

[11] DAS S, DATTA S, BASU D, DAS G C. Thermal cyclic behavior of glass-ceramic bonded thermal barrier coating on nimonic alloy substrate [J]. Ceramics International, 2009, 35: 2123−2129.

[12] AHMANIEMI S, VUORISTO P, MÄNTYLÄ T, CERNUSCHI F, LORENZONI L. Modified thick thermal barrier coatings: Thermophysical characterization [J]. Journal of the European Ceramic Society, 2004, 24: 2669−2679.

[13] YU Q, RAUF A, WANG N, ZHOU C. Thermal properties of plasma-sprayed thermal barrier coating with bimodal structure [J]. Ceramics International, 2011, 37: 1093−1099.

[14] CERNUSCHI F, AHMANIEMI S, VUORISTO P, MÄNTYLÄ T. Modelling of thermal conductivity of porous materials: Application to thick thermal barrier coatings [J]. Journal of the European Ceramic Society, 2004, 24: 2657−2667.

[15] ZHAO H, YU F, BENNETT T D, WADLEY H N G. Morphology and thermal conductivity of yttria-stabilized zirconia coatings [J]. Acta Materialia, 2006, 54: 5195−5207.

[16] CERNUSCHI F, BISON P, MOSCATELLI A. Microstructural characterization of porous thermal barrier coatings by laser flash technique [J]. Acta Materialia, 2009, 57: 3460−3471.

[17] PARKER W J, JENKINS R J, BUTLER C P, ABBOTT G L. Flash

method of determining thermal diffusivity, heat capacity, and thermal conductivity [J]. Journal of Applied Physics, 1961, 32: 1679−1684.
[18] PALIT S R. Elementary physical chemistry [M]. 30th edition. Calcutta: Book Syndicate Private Limited, 2001.
[19] RAVICHANDRAN K S, AN K, DUTTON R E, SEMIATIN S L. Thermal conductivity of plasma sprayed monolithic and multilayer coatings of Al_2O_3 and ZrO_2 [J]. Journal of the American Ceramic Society, 1999, 82: 673−682.
[20] KIM Y D, OH N L, OH S T, MOON I H. Thermal conductivity of W−Cu composites at various temperatures [J]. Materials Letters, 2001, 51: 420−424.
[21] BUENO L A, DONOSO J P, MAGON C J, KOSACHI I, DIAS FILFO F A, TAMBELLI C C, MESSADDEQ Y, RIBEIRO S J L. Conductivity and ^{19}F NMR in $PbGeO_3$−PbF_2−CdF_2 glasses and glass-ceramics [J]. Journal of Non-Crystalline Solids, 2005, 351: 766−770.

玻璃−陶瓷基粘接层热障涂层体系的热学性能

S. GHOSH

Bio-ceramics and Coating Division, CSIR–Central Glass and Ceramic Research Institute, Kolkata 700032, India

摘　要：研究了 8YSZ/BaO−MgO−SiO_2 玻璃−陶瓷/Ni 基合金热障涂层体系的热学性能。在相同条件下，热障涂层体系的热扩散系数和导热系数均比基底和只有玻璃−陶瓷涂层时的小。热障涂层体系的比热容、热扩散系数和导热系数随着温度的增加而增大，而导热系数随表层涂层厚度的增加而减小。

关键词：玻璃−陶瓷涂层；热障涂层；热学性能；氧化钇稳定氧化锆

(Edited by Yun-bin HE)